

1 **Validation of a Robust Method for Quantification of**
2 **Three-Dimensional Deformation of the Thoracic Aorta**
3 **Using Diffeomorphic Image Registration**

4 Zhangxing Bian^{1,2}, Jiayang Zhong^{1,2}, Jeffrey Dominic^{1,2}, Gary E.
5 Christensen³, Charles R. Hatt^{1,4}, and Nicholas S. Burris^{1,5}.

6 1. Department of Radiology, University of Michigan

7 2. Department of Electrical Engineering and Computer Science, University of Michigan

8 3. Department of Electrical and Computer Engineering, University of Iowa

9 4. Imbio, LLC

10 5. Department of Biomedical Engineering, University of Michigan

11 Version typeset February 21, 2021

12 Correspondence author: Nicholas S. Burris. Email: nburris@med.umich.edu

13
14 **Abstract**

15 **Purpose:** Accurately assessing thoracic aortic aneurysm growth is important. Maxi-
16 mal aortic diameter is the primary metric that is used to assess growth, but it suffers
17 from substantial measurement variability. The recently proposed method, Vascular
18 Deformation Mapping (VDM), quantifies three-dimensional aortic growth using an
19 approach based on deformable image registration. However, VDM has not yet been
20 validated to support the improved accuracy of VDM-derived measurements compared
21 to standard of diameter assessments.

22 **Methods:** Thus, we created a group of synthetic cases with great diversity to
23 systematically test and validate the robustness of VDM under a variety of variables
24 that influence clinical CTA data, such as respiratory motion, slice thickness and image
25 noise. Furthermore, by comparing the VDM-derived measurement with the manual
26 measurement from two perspectives – the accuracy and localization ability of maximal
27 diameter change, we demonstrate the superiority and practical use of our method on
28 clinical growth assessments.

29 **Results:**

30 **Conclusions:**

32 Contents

33	I. Introduction	1
34	II. Methods	2
35	II.A. VDM Registration	2
36	II.B. Create Synthetic Deformation	3
37	II.C. Maximal Diameter Measurement: Raters v.s. VDM	5
38	III. Results	6
39	III.A. Test VDM with AreaRatio	6
40	III.B. Comparison: VDM v.s. Raters	7
41	Appendix	9
42	References	9

43 1. Introduction

44 The thoracic aorta is the largest artery in the body, carrying blood from the heart to the
45 rest of the systemic circulation. A variety of degenerative and inflammatory processes cause
46 degrade the structural integrity of the normally elastic aortic wall resulting in thoracic aor-
47 tic aneurysm (TAA). Aneurysms of the thoracic aorta are often asymptomatic and indolent,
48 either remaining stable or growing slowly over a period of years or decades; however, a small
49 fraction of patients experience acute complications such as rapid growth, aortic dissection
50 or aortic rupture, all of which necessitate urgent surgical repair and are potentially fatal.
51 Current clinical guidelines recommend routine imaging surveillance of TAA and surveillance
52 regimens typically consist of annual or biannual computed tomography angiography (CTA)
53 examinations to assess for interval growth for other aortic complications. Maximal aortic
54 diameter is the primary metric that is used to assess growth and determine candidacy for sur-
55 gical repair, with measurements typically performed either manually or in a semi-automated
56 fashion using analysis software that allows for multi-planer or centerline based measurements
57 in planes orthogonal to the aortic axis.

58 Despite optimal measurement technique and operator experience, current diameter mea-
59 surement techniques are associated with substantial measurement variability – on the order
60 of ± 2 -5 mm – often limiting confident assessment of aortic growth at typical aortic growth
61 rates (< 1 mm per year). There are many potential sources of error/variability with diameter
62 measurements, however, common issues involve differences in measurement location along
63 the length of the aorta, differences in angulation of the 2-dimensional measurement planes,
64 and differences in radial position of the diameter calipers (especially when the aortic cross-
65 section is non-circular/elliptical). Without improved methods to measure aortic growth,
66 confident determination of disease progression, accurate assessment of patient risk and fully
67 informed treatment decisions will not be possible.

68 To address this problem, our group has recently proposed a method, termed Vascular
69 Deformation Mapping (VDM)[?], to quantify aortic growth in a more accurate and compre-
70 hensive fashion using an approach that employs deformable image registration to quantify
71 three-dimensional changes in the aortic wall morphology using high-resolution volumetric
72 computed tomography angiography (CTA) data. Preliminary reports of shown that the
73 VDM technique may be useful for more complete depiction of the extent of TAA growth
74 to inform surgical planning and for the assessment of growth during imaging surveillance,
75 however, the VDM approach and key algorithms have not yet been validated in a manner to
76 that supports the improved accuracy of VDM-derived measurements compared to standard
77 of care diameter assessments. While b-spline based techniques for deformable image regis-
78 tration are well-validated, and can achieve submillimeter registration accuracy using clinical
79 CT data, a variety of factors related to physiologic motion and image reconstruction may
80 influence the accuracy of registration results between serial aortic CTA examinations, and
81 thus a comprehensive evaluation of the influence of these factors is warranted.

82 The aim of this study was twofold: 1) examine the influences of a variety of variables
83 that influence clinical CTA data such as respiratory motion, slice thickness and image noise

84 on the accuracy of VDM-derived deformation assessment using a representative sample of
 85 synthetic CTAs, and 2) compare the accuracy of growth measurements between VDM and
 86 experienced manual raters using synthetic phantoms to better quantify the potential benefit
 87 on clinical growth assessments.

88 II. Methods

89 In this section, we will first introduce the VDM registration pipeline and the procedure
 90 to create the synthetic cases for testing the VDM. Then, we elaborate the approach of
 91 comparing the manual measurement and VDM-based measurement on the clinical task –
 92 measuring the maximal diameter change.

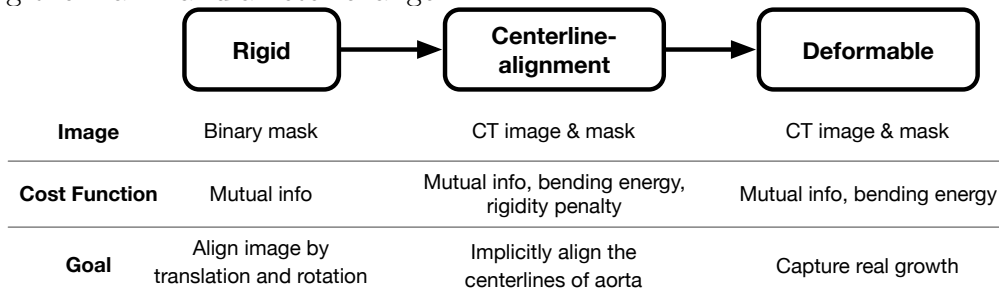


Figure 1: The registration pipeline.

93 II.A. VDM Registration

94 Given two CT images, we use the VDM, a deformable image registration pipeline, as shown
 95 in Fig.1, to capture the deformation of the aortic wall. The registration consists of three main
 96 steps: rigid, centerline-alignment, and deformable registration. The rigid registration only
 97 uses the mask of the aorta to rigidly align the images; the centerline-aligning and deformable
 98 registration use a multi-image multi-cost strategy, with each pair of images focusing on a
 99 different cost. Specifically, centerline-aligning, which can be more formally stated as highly-
 100 regularized deformable image registration with aortic rigidity penalty, will help align the
 101 centerlines of the aortas implicitly, allowing the later deformable registration to only focus
 102 on growth, without needing to fix any bulk motion or affine scaling. The aorta in the moving
 103 image will still move rigidly as in rigid registration, but the remaining areas of the moving
 104 image outside the aorta can move in a non-linear manner, which will help align the aortas
 105 more precisely. The last step, deformable registration, performs B-spline-based registration
 106 to capture the real growth.

107 During the registration, three cost functions involve – mutual information, bending en-
 108 ergy, and rigidity penalty. Mutual information¹ is a widely used metric in image registration
 109 to measure the image similarity; bending energy² is used to penalize the sharp changes in
 110 the deformation field and regularise the nonrigid transformation; and rigidity penalty³ will

111 penalize the large deformation and can be used to enforce a part of image transform in a
 112 rigid manner when using with a mask. The registration tool we used is Elastix⁴.

113 II.B. Create Synthetic Deformation

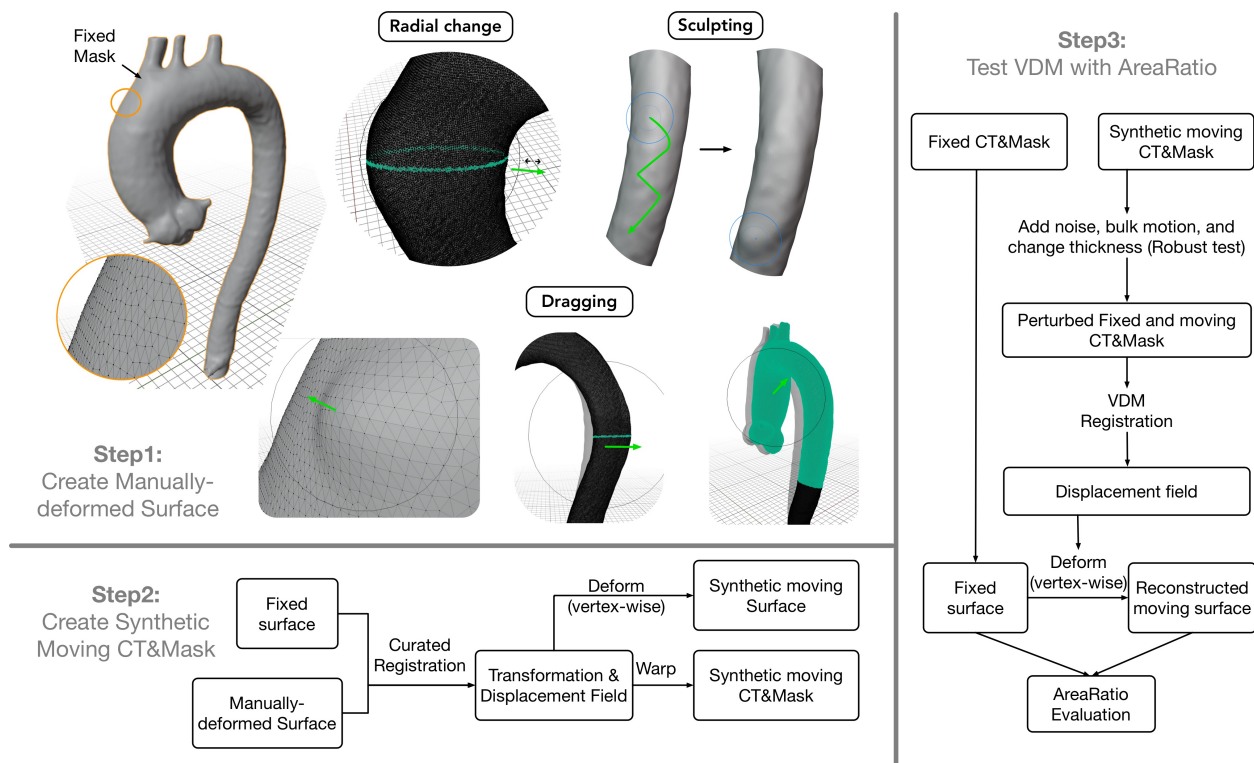


Figure 2: The pipeline for creating synthetic images and validation process with AreaRatio. In step1, we use three ways to create the deformations on 3D meshes, which are radial changing, sculpting, and dragging. In step2, we take the manually-deformed surface to a curated registration process and use the resulting transformation to warp the CT and mask to obtain the synthetic images, and use the displacement field to deform the fixed surface to create the synthetic moving surface. In Step3, we test our VDM registration pipeline using synthetic images with various disturbances. We deform the fixed surface by the resulting displacement field from VDM registration and compare the AreaRatio against the ground-truth AreaRatio computed from the fixed surface and synthetic moving surface. The results of registration and robust test can be found in Fig.4.

114 **Step1: create manually-deformed surface.** We first build the 3D fixed surface from
 115 the fixed image’s mask, and then we use the Blender (www.blender.org), an open-source 3D
 116 modeling software to create synthetic deformation. In this paper, we use the vertex-vertex
 117 type mesh, meaning a mesh can be presented by of a set of vertices $\mathcal{V} = v_1, v_2, \dots, v_N$, and
 118 each face is constructed by three vertices and can be written as $f_{\{v_i, v_j, v_k\}}$. Each vertex
 119 v_i has a position (x_i, y_i, j_i) in the 3D space. When making manual deformation to the
 120 surface using Blender, we change the position of a few vertices, and we denotes the vertices

121 in deformed surface as $\tilde{\mathcal{V}}$ and note that the vertex-wise correspondence is maintained, i.e.
 122 $v_i \leftrightarrow \tilde{v}_i, v_i \in \mathcal{V}, \tilde{v}_i \in \tilde{\mathcal{V}}$. Since a surface can be represented by a set of vertices, for convenience,
 123 we will simply use the same notation to represent surface, for example, \mathcal{V}_{fixed} representing
 124 the fixed surface.

125 We created 31 synthetic cases in various locations on the aorta and with various degrees
 126 of deformation (the displacement magnitudes range from 0-7mm), which cover most situa-
 127 tions we observed in the real clinical scenario, to guarantee the diversity of our synthetic
 128 dataset. For example, we created the manually-deformed surface in three ways, with each
 129 mimicking a scenario: radial changing mimics the aortic aneurysm growth in the radial di-
 130 rection; sculpting mimics some random irregular deformation and the bulge with strip shape,
 131 which often develops in descending aorta; and dragging single vertex or a group of vetices
 132 can give examples of local growth, bending, longitudinal stretch, and respiratory effect.

133 **Step2: create synthetic moving CT&Mask.** This step aims to obtain the synthetic
 134 moving surface and synthetic moving CT&Mask given the manually-created surface. We
 135 perform a curated registration procedure on the fixed surface and manually-deformed surface
 136 to generate the transformation that can be used to warp the fixed image/mask to obtain
 137 synthetic moving image/mask and the displacement field that can be used to vertex-wisely
 138 deform the fixed surface \mathcal{V}_{fixed} to obtain the synthetic moving surface \mathcal{V}_{moving} . Specifically,
 139 we construct a binary image where the voxel that contains any vertex is one (otherwise zero)
 140 for both fixed and manually-deformed moving surfaces. These two binary images indicate
 141 the silhouette of the aorta, so we refer to them as boundary images. Then we register these
 142 two boundary images and use the resulting transformation to warp the fixed CT and mask to
 143 obtain the synthetic images, and also use the resulting displacement field to deform the fixed
 144 surface to create the synthetic moving surface. Note that the fixed surface and the synthetic
 145 moving surface have vertex-wise correspondence, which allows us to compute the AreaRatio
 146 for each face. We take the AreaRatio computed from \mathcal{V}_{moving} and \mathcal{V}_{fixed} as ground truth for
 147 the later evaluation step (Step3 in Fig.2).

148 **Step3: Test VDM with AreaRatio.** After obtaining the synthetic moving im-
 149 age&mask, we take the fixed image&mask and synthetic moving image&mask to test our
 150 VDM registration under various disturbances which can be encountered in the real clinical
 151 scenarios, such as image noise, bulk motion, and various thickness of the image slice. We
 152 take the AreaRatio as the metric to measure the registration performance.

153 AreaRatio is defined as the ratio of the area of a face in one mesh to that of the
 154 corresponding face in another mesh.

$$155 \quad AreaRatio_f = \frac{S(f_{\{\tilde{v}_i, \tilde{v}_j, \tilde{v}_k\}})}{S(f_{\{v_i, v_j, v_k\}})}, \quad (1)$$

156 where the $S(\cdot)$ indicates the area of a face. The reasons we prefer using AreaRatio
 157 over the Jacobian determinant are three-fold: (1) the AreaRatio is more straightforward and
 158 intuitive to represent surface expansion and compression. (2) the visual effect of AreaRatio
 159 plot is more consistent with the humans' perception of growth (deformation) when plotting

160 the values onto the surface. (3) ???

161 After registration, we take the resulting displacement field to vertex-wisely deform the
 162 fixed surface \mathcal{V}_{fixed} to get reconstructed moving surface \mathcal{V}_{recons} and compare the AreaRatio
 163 against the ground truth AreaRatio that are computed by \mathcal{V}_{fixed} and \mathcal{V}_{moving} . The results
 164 are reported in Section.III.A..

165 II.C. Maximal Diameter Measurement: Raters v.s. VDM

166 In this section, we focus on the clinical task, i.e., measuring the maximal diameter change
 167 (representing the maximal deformation), and introduce the procedure used to compare VDM-
 168 based measurement and manual measurement.

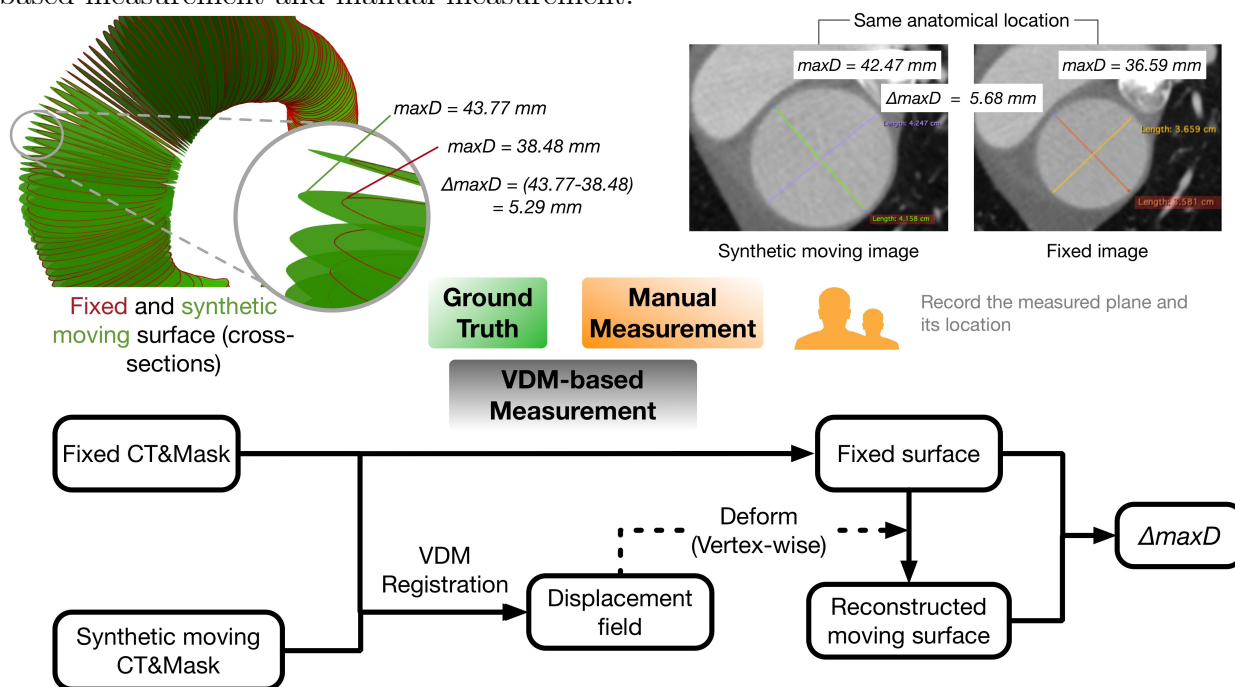


Figure 3: Validation process on maximal diameter change.

169 We invite two experienced raters to measure the maximum deformation (i.e., the maxi-
 170 mal diameter change) following the common practice and record three points in the measured
 171 plane. During the measurement, raters put the synthetic moving image and fixed image side
 172 by side and try their best to locate the position where the maximum deformation appears
 173 while keeping the measured plane corresponding to the same anatomical location. Since
 174 the other parts of the CT image rarely change, which provides raters with clear landmarks,
 175 finding the same anatomical location and maximal diameter change can be a much easier
 176 task than in real clinical scenarios. Thus, the rater’s performance on the synthetic cases is
 177 considered as the upper bound that manual measurement can possibly achieve.

178 To get the ground-truth maximal diameter change, we first extract the centerline of
 179 the fixed image and sample the centerline with 0.5mm spacing and the maximum diameter
 180 of each cross-section (orthogonal to the centerline) at each sampled point in both fixed
 181 surface and synthetic moving surface is automatically computed by the open-source Vascular
 182 Modeling Toolkit (VMTK, www.vmtk.org). We denote the results as two one-dimensional
 183 arrays $\mathbf{d}_{\mathcal{V}_{fixed}}$ and $\mathbf{d}_{\mathcal{V}_{moving}}$, with each having the length of the number of samples on the
 184 centerline. Then we take $\max(|\mathbf{d}_{\mathcal{V}_{fixed}} - \mathbf{d}_{\mathcal{V}_{moving}}|)$ as the ground-truth maximal diameter
 185 change and record the location of the cross-section that achieves the maximal diameter
 186 change.

187 In the VDM-based measurement, we obtain the reconstructed moving surface by de-
 188 forming the fixed surface using the displacement field resulting from registering the original
 189 CT image and synthetic moving image. Similarly, we take the same sampled centerline and
 190 measure the maximum diameter of cross-sections for both fixed surface and reconstructed
 191 moving surface, and record the largest difference (i.e., $\max(|\mathbf{d}_{\mathcal{V}_{fixed}} - \mathbf{d}_{\mathcal{V}_{recons}}|)$) and location
 192 where it happens.

193 We compare VDM-based and manual maximal diameter measurement against the
 194 ground truth, and the results can be found in Section III.B..

195 III. Results

196 III.A. Test VDM with AreaRatio

197 **Robust Test.** We test our VDM registration method with three types of disturbance, image
 198 noise, various thickness of the image slice, and bulk motion. These sub-ideal scenarios can
 199 always be seen in real clinical settings. We add various Gaussian noise levels for noise attack,
 200 with the magnitude of 50, 100, and 150 (in HU), to the CT image before VDM registration.
 201 Also, to test the robustness of VDM to various thicknesses of image slice (in the z-direction),
 202 we resample the image using three thicknesses: 1.0, 1.5, and 2.0 (mm). Furthermore, to
 203 mimic the bulk motion, we rotate the image along three axes by randomly selecting from
 204 $\{+5, -5\}$ degree and translate the image to the direction $(+x, +y, +z)$ by various distances,
 205 20, 40, 60 (mm). The results in Fig.4 shows that VDM is robust to various disturbances.

206 **Test on Respiratory Effect.** Whenever taking CT scans, a patient can't hold their
 207 breath at the same level, which leads to the respiratory effect. Besides the 31 synthetic cases
 208 that mainly focus on the local deformation, we created another 4 cases with respiratory effect
 209 to test VDM. Fig.5 shows VDM can perform well on such cases and achieve low error on
 210 AreaRatio.

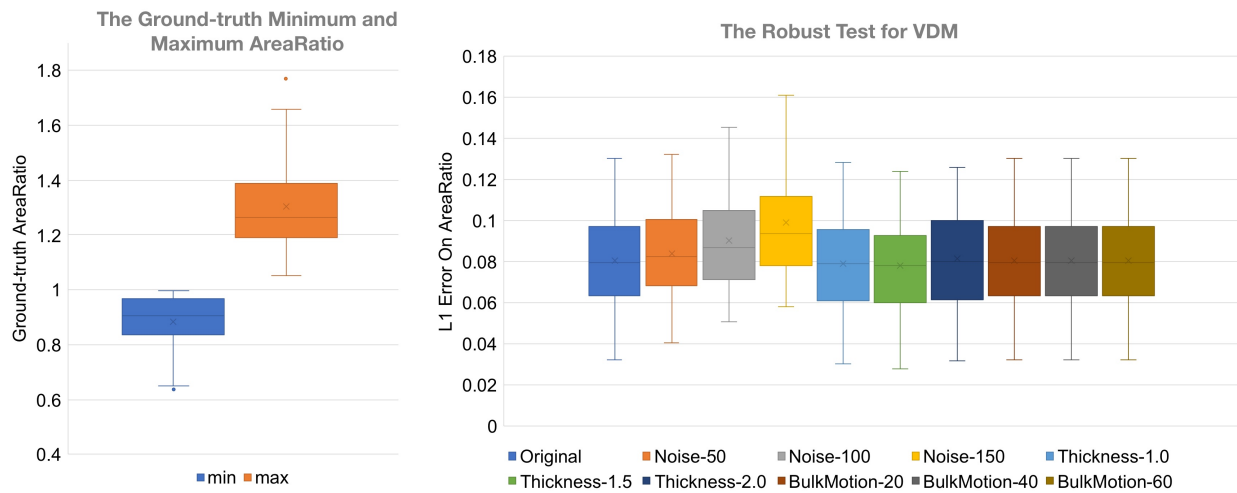


Figure 4: The left figure shows the statistics of the max and min value of the AreaRatio for the 31 synthetic cases. In the right plot, the “original” indicates the test with the original CT image and mask w/o any disturbance. For the rest of the test, we add one and only one disturbance to the original image pair to test the VDM. The 95th percentile of L1 error on AreaRatio is reported.

211 **III.B. Comparison: VDM v.s. Raters**

212 Following the procedure described in Fig.3, we compare VDM-based measurement with
 213 manual measurement from two aspects to show our superiority – the variability of the mea-
 214 surement and the ability to locate the region where the maximal diameter change happens.
 215 Fig.6 shows the VDM-based measurement achieve much smaller variability than that of both
 216 raters, and also shows more accurate localization for maximal diameter change.

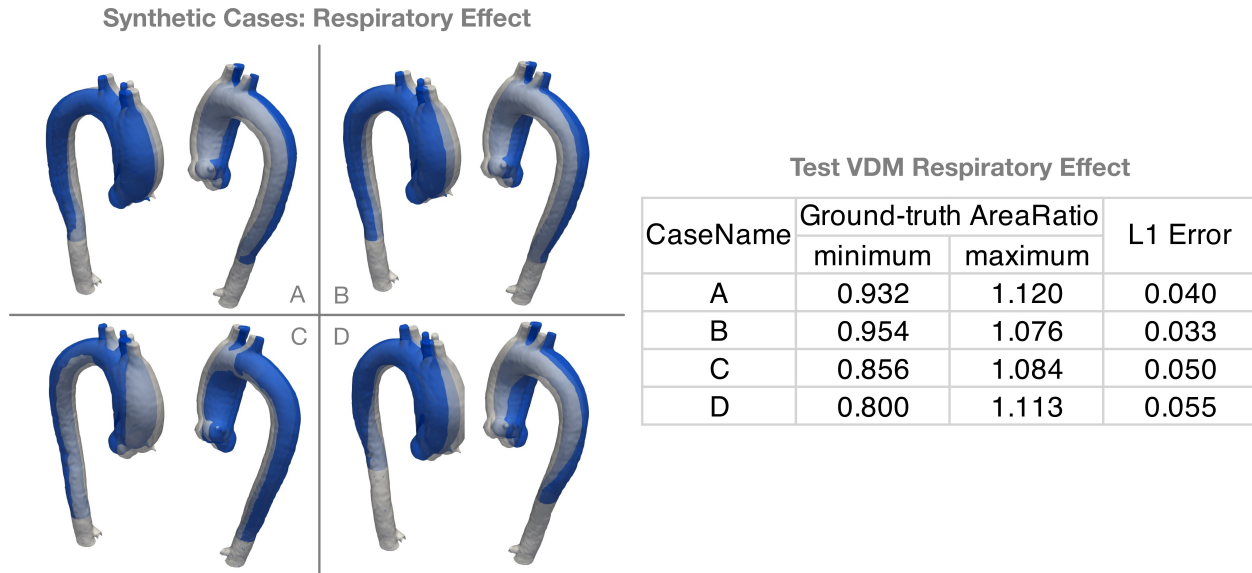


Figure 5: On the left, we show four synthetic cases created for testing respiratory effect with two angle of views each. The white surface is fixed surface while the blue surface is the synthetic moving surface. On the right, we reported the statistics of the ground-truth AreaRatio and the 95th percentile of L1 error on AreaRatio.

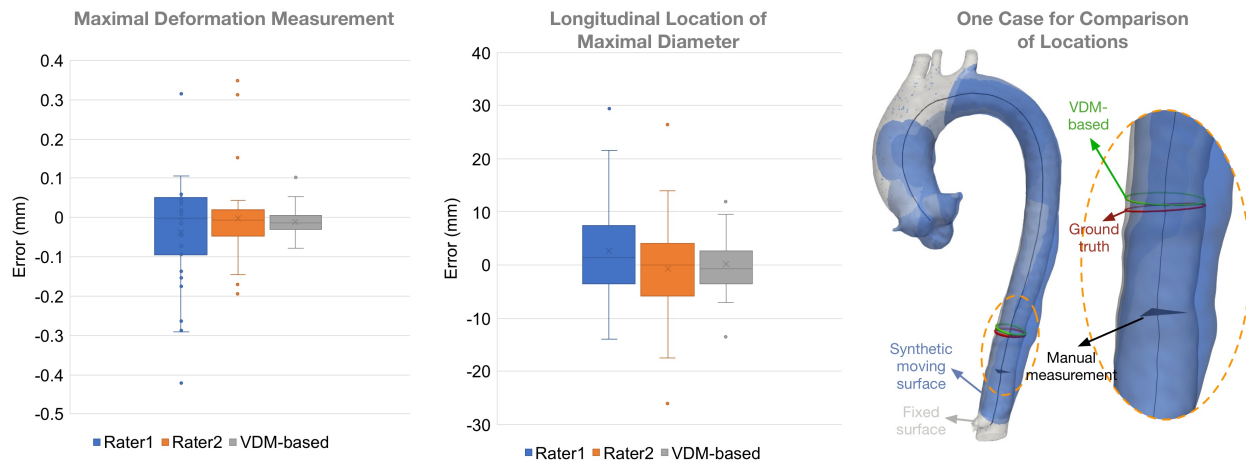


Figure 6: Two box-plots on the left show the error of maximal deformation and longitudinal localization by two raters and the VDM-based method. The right figure gives an example of the three locations: ground-truth location, the one found by rater1, and the one found by the VDM-based measurement.

217 Appendix

218 Appendix text goes here if needed.

220 References

- 221 ¹ P. Thévenaz and M. Unser, Optimization of mutual information for multiresolution image
222 registration, *IEEE transactions on image processing* **9**, 2083–2099 (2000).
- 223 ² M. Staring and S. Klein, Itk: Transforms supporting spatial derivatives, *Insight J* (2010).
- 224 ³ M. Staring, S. Klein, and J. P. Pluim, A rigidity penalty term for nonrigid registration,
225 *Medical physics* **34**, 4098–4108 (2007).
- 226 ⁴ S. Klein, M. Staring, K. Murphy, M. A. Viergever, and J. P. Pluim, Elastix: a toolbox
227 for intensity-based medical image registration, *IEEE transactions on medical imaging*
228 **29**, 196–205 (2009).